Oblique sputtering of amorphous TbFeCo thin films on glass substrates and the effect of deposition angle on perpendicular magnetic anisotropy

Cite as: Journal of Applied Physics **81**, 3555 (1997); https://doi.org/10.1063/1.364959
Submitted: 05 January 1996 . Accepted: 31 December 1996 . Published Online: 04 June 1998

Yung-Chieh Hsieh, Sergei Gadetsky, Takao Suzuki, and M. Mansuripur

Oblique sputtering of amorphous TbFeCo thin films on glass substrates and the effect of deposition angle on perpendicular magnetic anisotropy

Yung-Chieh Hsieh[a] and Sergei Gadetsky
Optical Sciences Center, University of Arizona, Tucson, Arizona 85721

Takao Suzuki
Toyota Technological Institute, Nagoya, Japan

M. Mansuripur
Optical Sciences Center, University of Arizona, Tucson, Arizona 85721

(Received 5 January 1996; accepted for publication 31 December 1996)

We measured the magnetic hysteresis loops for several obliquely deposited amorphous TbFeCo films. The experimental results show that the direction of the average magnetic anisotropy (i.e., the easy axis of magnetization) is no longer along the surface normal. With the help of computer simulations, we have quantified the effects of oblique deposition in terms of the deviations of local anisotropy directions from the surface normal. We also found that, with the increasing of the deposition angle, the compensation point shifts toward the Fe-rich side and the films become thinner. © *1997 American Institute of Physics.* [S0021-8979(97)04607-0]

I. INTRODUCTION

In magneto-optical (MO) disks, a thin magnetic film is deposited on a substrate patterned with grooves, lands, and preformat marks. In the land region, the average direction of magnetic anisotropy is along the disk's surface normal due to the fact that the direction of film deposition on average is perpendicular to the land surface. However, on the sidewalls of grooves and pits, the average direction of sputtering and the wall's normal direction make an angle θ with each other; this might cause the distribution of the easy axes on these sidewalls to develop a certain degree of asymmetry with respect to the normal direction.

In a previous article,[1] we showed that variations of the anisotropy direction and/or the magnetic film thickness on the sidewalls could contribute to the pinning of the magnetic domain walls in these regions. This pinning phenomenon has also been exploited as a possible mechanism for enhancing data storage density in MO recording.[2,3] Further progress in the application of this technique requires a better understanding of the magnetic properties of the films in the side wall region.

In this article, we concentrate on studying the effect of oblique deposition on the distribution of the magnetic anisotropy axis, which is directly related to the magnetic properties of patterned MO disks.[3] A few articles on this subject have been published previously. Hong *et al.* measured the distribution of easy axes of a dc getter sputtered amorphous Gd–Co film using a torque curve method.[4] Togami *et al.* pointed out that there is considerable dispersion in the orientation of the easy axes of magnetization in sputtered amorphous Gd–Tb–Fe alloy films, and that their dispersion brings about the decrease of the Kerr rotation angle.[5] They also concluded that the dispersion depends on the bias voltage applied to the substrate during deposition. Hellman *et al.* investigated the source of unidirectional anisotropy by employing the exchange coupling between amorphous TbFe film and a permalloy film, and showed that the direction of easy axis in an obliquely deposited sample makes a small angle to the film normal.[6] They proposed that the origin of the tilt of the easy axis is related to the direction of incidence of the Tb and Fe atoms during deposition. In their later work,[7] the dependence of the effective easy axis direction on deposition temperature, the incidence angles of Tb and Fe atoms, the film's composition, and thickness, etc. were studied based on torque magnetometry (In these experiments, the incident angles of Tb and Fe were on opposite sides of the film normal.). They concluded that the magnetic anisotropy energy for obliquely deposited Fe-rich material grown at room temperature requires, instead of a simple uniaxial form, a more complex form containing two different angles.

Comparing our work reported here with that of earlier authors,[4–7] there are, at least, the following differences: (1) The incident angle of deposition in our samples can be as large as 80 deg, and both Tb and Fe are deposited nearly from the same direction. (2) Instead of measuring torque curves, we measured the hysteresis loops using a Kerr loop tracer. Several complementary pieces of information are obtained by applying the magnetic field in different directions. (3) Explanation of the torque data in the past has been based on the Stoner–Wohlfarth coherent rotation model, which ignores the effects of patchiness of the thin-film media.[8] In our analysis, we have assumed that our amorphous films consist of islands or patches of material, coupled to each other via exchange forces at the patch boundaries. Based on computer simulations, we have found it impossible to explain all the experimental data without introducing the concept of patches.

The scope of this article is as follows. In Sec. II, we present the experimental hysteresis loops obtained by applying the magnetic field either parallel or perpendicular to the film's surface, and discuss the possible modes of magnetiza-

[a]Electronic mail: hsieh@aruba.ccit.arizona.edu

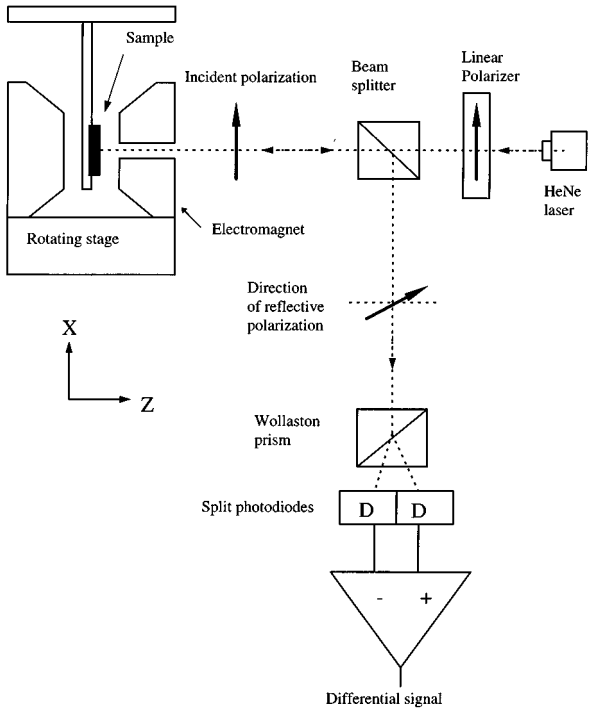

FIG. 1. Schematic diagram showing the loop tracer used in our study. A linearly polarized laser beam is incident on the sample whose normal is along the Z axis. With the help of differential detector, one can measure the Kerr-rotation angle of the reflected light, which carries information about the sample's state of magnetization. Note that the magnetic field is perpendicular to the sample's surface in the figure. In addition, we can rotate the electromagnet by 90° to apply an in-plane field.

tion reversal behind the data. Section III gives results of computer simulations in which we have assumed that the film consists of several patches and that the anisotropy axes have an asymmetric distribution around the surface normal of the film. It will be seen that very good qualitative agreement is obtained between theory and experiment in all cases considered.

II. EXPERIMENTAL RESULTS AND DISCUSSION

In this study, we used a Kerr loop tracer to measure the Kerr-rotation angles, hysteresis loops, and magnetic anisotropy curves of the obliquely deposited magnetic films. The experimental set up is shown in Fig. 1. Samples measured in our experiments were deposited by magnetron sputtering using two different targets of Tb and FeCo. The distance from the targets to substrate is about 5 in., and that between two targets is 1.5 in. In our studies, four sets of samples were measured. Each set included five samples which were deposited at normal incident (θ=0°) and at the oblique angles of θ=20, 40, 60, and 80°. Different sets of samples had different thicknesses; for instance, the films deposited at normal incidence had thicknesses of 25, 30, 50, and 60 nm in the four sets. Within each set, the thickness of the magnetic film decreased with the increasing angle of deposition. The reduced thickness was visible to the naked eye as the transparency of the samples increased at larger angles of deposition. However, we did not make a quantitative measurement of

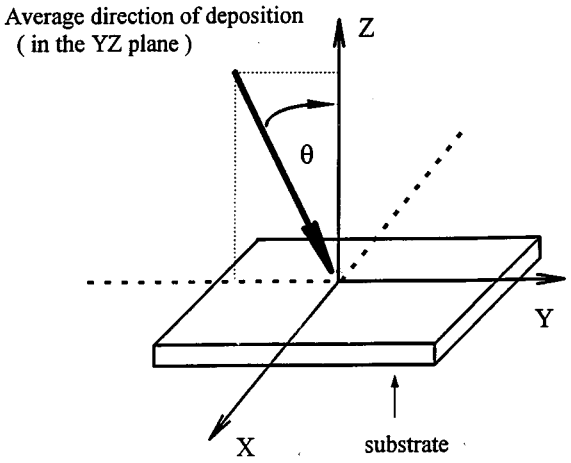

FIG. 2. Schematic diagram showing the geometry of oblique-deposition by sputtering. The film's normal is along the Z axis and the average direction of sputtering is in the YZ plane toward $-Y$, making angle θ with the Z axis.

the various films' thicknesses. All samples were coated *in situ* with a protective layer of SiN. Since the magnetic measurement results for the four sets are qualitatively the same, we discuss here the results obtained from one of the sets only. (This is the set in which the sample deposited at normal incidence was 50 nm thick.)

We define $+\mathbf{Z}$ as the direction of film's normal, and H_x, H_y, and H_z as the components of the magnetic field applied along $+\mathbf{X}$, $+\mathbf{Y}$, and $+\mathbf{Z}$ directions. As shown in Fig. 2, the sputtering direction is in the YZ plane, making an angle θ with $\mathbf{Z}$. Before each measurement, the magnetization of the film was saturated along $+\mathbf{Z}$ and then allowed to relax in zero field.

A. Magnetic field applied along the *Z* direction

Figure 3 shows several hysteresis loops obtained by applying the magnetic field along Z for samples deposited at different angles θ. We observe that, as θ increases from 0 to 80°, the films, which originally are Tb rich, show an enhanced coercivity because their composition approaches the compensation composition, and eventually become Fe rich somewhere between θ=60 and θ=80°. One possible explanation of this phenomenon is that the larger size of the deposited Tb atoms gives a larger cross section for resputtering from the film surface. In other words, the resputtering rate of Tb is higher than that of Fe, which causes that the composition at large deposition angle moves towards the Fe-rich side.

In Fig. 3, near H_z=0, the slopes of curves (a)–(c) remain fairly small, thus, indicating that the magnetization vector after relaxation is along Z direction. It turns out that the anisotropy easy axis could not deviate from Z axis coherently in a significant angle. However, in Fig. 3(d), corresponding to θ=60°, we start to see the difference in Kerr signals for H_z=0 and H_z=20 kOe. The Kerr angle at H=0 is 20% less than that at H=20 kOe. This result might be caused by either the coherent deviation or the asymmetric distribution of anisotropy easy axis around the surface normal of the films. Investigations on the in-plane hysterisis loops given in

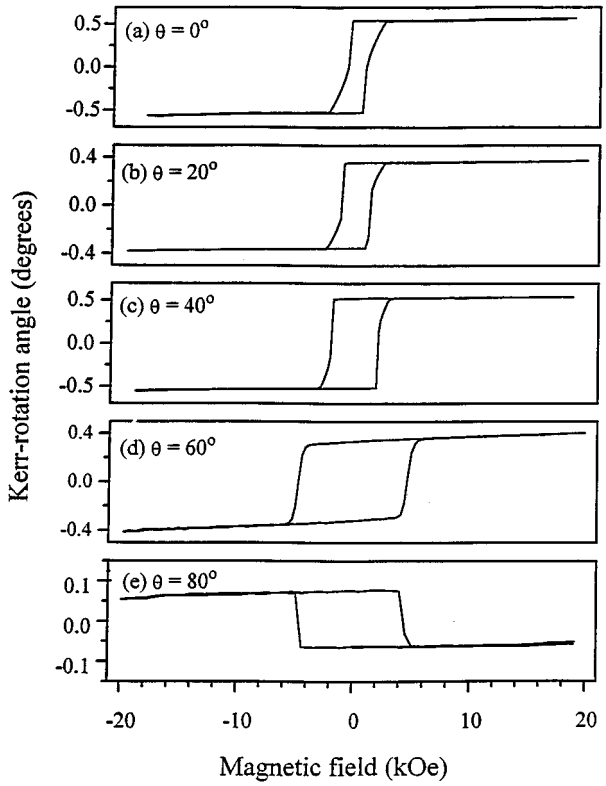

FIG. 3. Hysteresis loops obtained by applying the magnetic field along Z for samples deposited at different angles θ. When θ increases from 0 to 80°, the films, which originally are Tb rich, become Fe rich somewhere between θ=60 and 80°. The coercivity of the samples increases when their composition approaches the compensation composition.

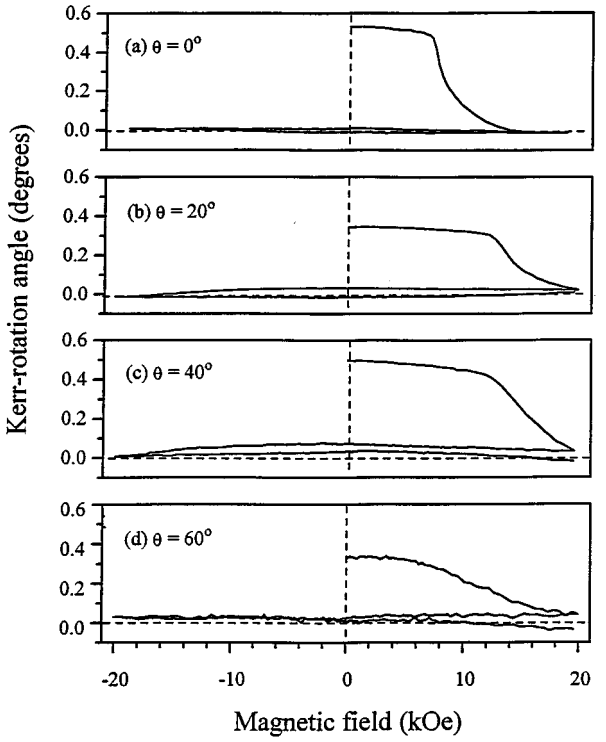

FIG. 4. Hysteresis loops obtained by applying the magnetic field along X for samples deposited at different angles. When H_x increases gradually, the various magnetic patches rotate coherently in the early stage, thus causing the slow decrease of the Kerr signal. After H_x exceeds a critical value [7 kOe in Fig. 4(a)], some of the patches reverse to form magnetic domains; the curvatures of the curves change sign at this point. Because the distribution of easy axes is symmetric with respect to the YZ plane, half of the patches are reversed when H_x is strong enough (20 kOe in our case). This causes the Kerr signal to become zero. At the same field, all the magnetic moments are pushed close to $+X$ direction. When H_x is reduced from its maximum value, patches within the up domains increase their $+Z$ component, while patches within the down domains increase their $-Z$ component. The Kerr signal, therefore, remains zero.

Secs. II B and C provide more information about the distribution of easy axis.

B. Magnetic field applied along the *X* direction

Figure 4 shows plots of Kerr signal versus H_x for samples deposited at θ=0, 20, 40, and 60°. (The curve for the sample deposited at θ=80° is not shown because it is similar to those for θ=40° and 60°). Note in Fig. 4(a) that the initial Kerr signal at H_x=0 is the same as that in Fig. 3(a). Upon increasing H_x gradually, it is observed that, up to the point where H_x=7 kOe, the curvature of the curve in Fig. 4(a) is negative, but it becomes positive beyond that point. The phenomenon can be understood as follows. A small in-plane field can only bend the magnetization away from $+Z$ coherently. Thus, the curve is an arc of an ellipse centered at the origin and has a negative curvature. When H_x reaches a critical value (H_{crit}=7 kOe in this case), some of the magnetic patches within the sample switch direction, so that the magnetization loses some of its $+Z$ component and gains some $-Z$ component. This causes the Kerr signal to exhibit a sharp drop at $H_x=H_{\text{crit}}$. Beyond H_{crit}, more and more regions break into domains, but now the magnetic moments are forced to approach the $+X$ direction. At H=15 kOe, two possibilities exist. One is that the area of the reversed domains (magnetization along $-Z$) within the film is equal to that of the nonreversed regions (magnetization along $+Z$), which causes the Kerr signal to go to zero. Beyond this point, no more reversals occur. Increasing the field only pushes the magnetic moments closer to the $+X$ direction, but the signal remains zero. When H_x is reduced from its maximum value, dipoles within the up domains increase their $+Z$ component, but dipoles within the down domains also increase their $-Z$ component. The total magnetization, therefore, continues to be zero. Another possible situation which might occur at H=15 kOe is that the field has already been strong enough to push all the magnetic patches to the $+X$ direction. In this case, the Z component of magnetization is equal to zero. Once H_x begins to decrease from its maximum value, the number of patches returning to $+Z$ would be the same as that switching to $-Z$. This is because the distribution of the anisotropy axes among the patches is symmetric with respect to the Z axis. Up to this point, all we can say is that at normal deposition the average anisotropy direction is coincident with the Z axis. Thus, when a strong in-plane field is applied, the film is demagnetized by breaking into equal areas of up and down magnetization.

Figures 4(b)–(d) show the corresponding curves for θ=20, 40, and 60°. The behavior of these loops is similar to that shown in Fig. 4(a). To explain these observations, we

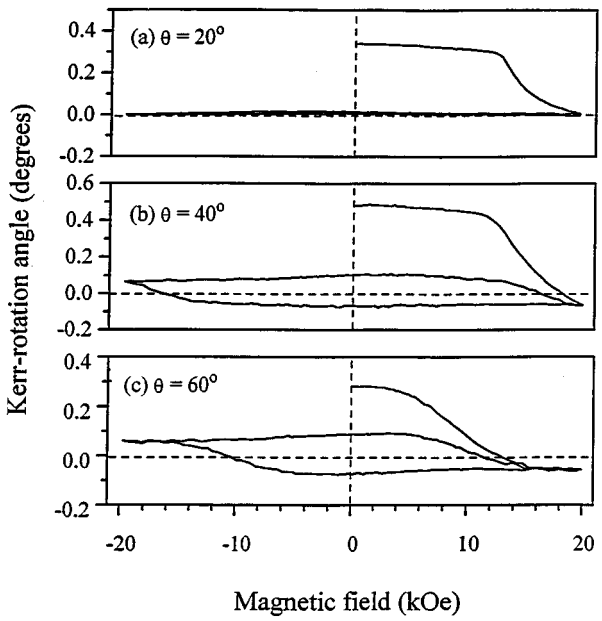

FIG. 5. Hysteresis loops obtained by applying the magnetic field along Y for samples deposited at different angles θ. (a) At $\theta=20°$, the sample does not show significant difference when its behavior is compared with that shown in Fig. 4(b). This indicates that the average direction of easy axis is still very close to Z, so that applying the field along X and Y does not make much difference. (b) At $\theta=40°$, the magnetization rotates coherently when the field is below 12 kOe. Beyond that point, some of the magnetic patches begin to reverse. At $H_y=20$ kOe, the Kerr signal is negative because the area of the down domains is larger than that of the up domains. When H_y changes from 20 to -20 kOe, all the patches flip and, therefore, the Kerr signal switches sign. (c) At $\theta=60°$, one observes the same qualitative behavior as (b).

must remember that the direction of sputtering and, consequently, the distribution of the anisotropy axes are symmetric with respect to the YZ plane; therefore, one cannot tell the difference between films deposited at different angles by applying the magnetic field along the X direction.

C. Magnetic field applied along the *Y* direction

Figures 5(a)–(c) show the loops obtained by applying the magnetic field along the Y direction for samples deposited at $\theta=20$, 40, and 60°, respectively. In Fig. 5(a), the curve has the same behavior as in Fig. 4(b). However, Figs. 5(b) and 5(c) show a different behavior when compared to the corresponding curves in Figs. 4(c) and 4(d). In these figures, after H_y reaches its maximum, the Kerr signals begin to show hysteretic behavior with the sweeping of the magnetic field. This behavior indicates that the average direction of magnetic anisotropy is no longer aligned with the Z axis, but that it is along some other direction in the YZ plane.

One of the possible scenarios that might explain the results shown in Fig. 5 is as follows. Let us separate the various magnetic patches of the sample into two groups: a symmetric group **S**, where for each given patch belonging to **S**, there exists a corresponding patch, also belonging to **S**, such that the anisotropy directions of the two patches are symmetric with respect to the Z axis. Those patches that are not in **S** comprise the second group called **A**. Note that the average anisotropy direction of the patches in **S** is along Z, but the average easy axis for patches in **A** is somewhere in the YZ plane toward $-Y$, making an angle with the Z axis whose value depends on θ. It is also reasonable to expect that the fractional area of patches in **A** is proportional to the ratio of the Kerr signal at $H_y=0$ to that in the saturated state. According to the data shown in Fig. 5, the majority of the patches belong to **S** until the deposition angle θ reaches 40°. When the average easy axis for all the patches is not too far away from Z, the strong exchange coupling among adjacent patches forces the direction of magnetization after relaxation from the saturated state to remain very close to the Z axis. Upon increasing H_y, the magnetic moments of the various patches begin to rotate coherently in the beginning. Afterwards, magnetization reversal occurs in some of the patches once H_y exceeds H_{crit}. In Fig. 5(b), the Kerr signal is zero at $H_y=18$ kOe, presumably because the areas of up and down domains are equal. At $H_y=20$ kOe, we speculate that all patches having an easy axis toward-Y are reversed. This means that roughly half the elements of **S** and all the elements of **A** have reversed. Therefore, the negative signal level at $H_y=20$ kOe arises from the patches in group **A** alone. After this point, the patches in **S** do not contribute to the Kerr signal; changing H_y from $+20$ to -20 kOe causes all patches to flip and, therefore, switch the sign of the Kerr signal.

Note that, at small deposition angles, almost all the patches belong to **S**. It turns out that the magnetic anisotropy can be well described by a uniaxial film whose easy axes are distributed within a range of angles around the film normal, but the average direction remains along $+Z$. This result is consistent with earlier work.[4,5] However, when the deposition angle becomes large, the average direction of the easy axis is no longer normal to the film's plane. This conclusion is in agreement with that reached by Hellman *et al.*[6,7]

III. COMPUTER SIMULATION RESULTS

In this Sec. III, we show computer simulation results obtained by assuming that the directions of easy axes have an asymmetric distribution. We use a one-dimensional lattice of 100 dipoles having uniaxial magnetic anisotropy and nearest neighbor exchange to simulate the effects of tilted easy axis. The simulation is based on the Landau–Lifshitz–Gilbert equation of magnetization dynamics as elaborated in Ref. 1 and 9. The following set of parameters were used throughout: saturation magnetization $M_s=100$ emu/cm^3, anisotropy constant $K_u=10^6$ erg/cm^3, exchange stiffness coefficient $A_x=5\times10^{-8}$ erg/cm, gyromagnetic ratio $\gamma=-10^7$ H_z/Oe dipole spacing or lattice constant $d=10$ Å, and viscous damping coefficient $\alpha=3$. In the simulations, we have considered that the magnitude of the magnetization M_s is uniform over a single film. We believed that it is a reasonable assumption even though the film is obliquely deposited. Also, note that M_s is the total magnetization; therefore when the composition changes with the deposition angle, M_s must be changed in the simulation. Since all the fields in simulations (anisotropy field, exchange field, and external field) are normalized by M_s,[9] variations of M_s change only the scale of these associated fields. For example, if we set $M_s=100$

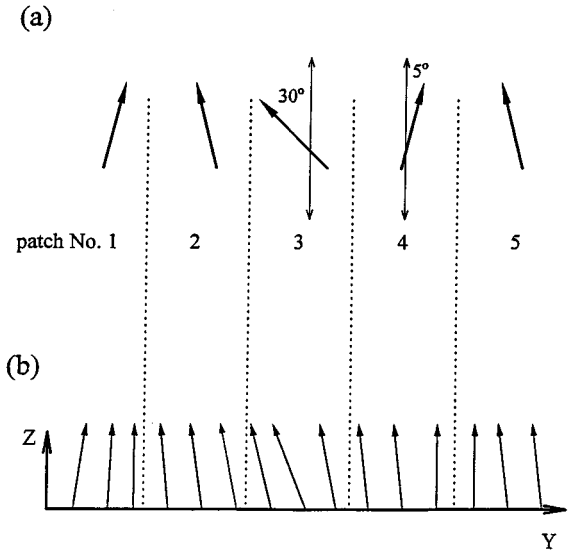

FIG. 6. (a) Distribution of local easy axes for the dipoles in simulation. (b) Schematic diagram showing magnetic dipoles in a one-dimensional lattice upon relaxation from the saturated state along $+Z$.

emu/cm^3, the computed coercivity H_c turns out to be 10 KOe, whereas with $M_s=50$ emu/cm^3, the computed coercivity will be 20 kOe.

In this simulation, the dipoles are grouped into five patches and the assumed directions of the local easy axes within each patch are shown in Fig. 6(a). Each patch contained 20 dipoles, and the exchange stiffness coefficient at the patch boundaries was set to only 20% of that between adjacent dipoles within the patches. The first and the fourth patch have their easy axes away from the Z axis by 5° toward $+Y$; the second and the fifth patch have their easy axes away from the Z axis by 5° toward $-Y$. The third patch is 30° away from Z toward $-Y$. We assume that the large deviation of the third patch is caused by the oblique deposition. As discussed in Sec. II C, the third patch belongs to group **A**, while the other patches belong to group **S**. Figure 6(b) shows the angular distribution of dipoles after relaxation from the saturated state. Due to strong exchange coupling, all the dipoles in Fig. 6(b) point more or less in the $+Z$ direction, even though the easy axis of the third patch has a significant deviation from Z.

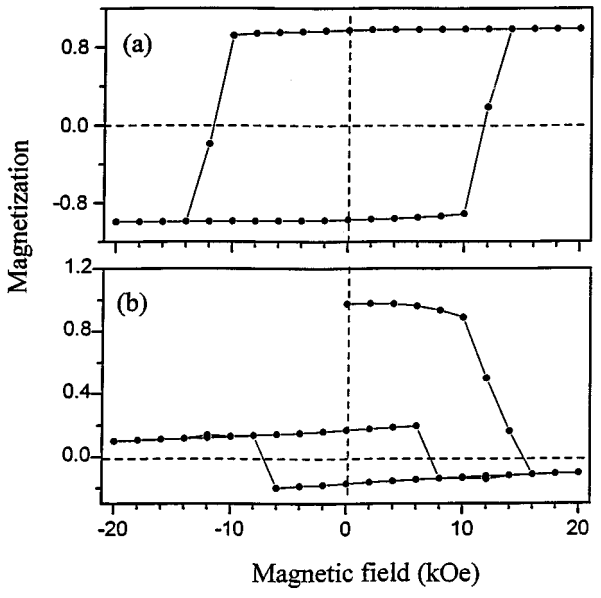

FIG. 7. Computed loops obtained by applying the magnetic field either perpendicular or parallel to the film's surface normal. (a) When the file is along the Z direction, magnetization remains more or less almost constant with the increasing of the magnetic field. This is in agreement with the measurement results shown in Figs. 3(b) and 3(c). (b) When the applied field is along the Y direction, the asymmetric behavior of the magnetization is similar to that shown in Figs. 5(b) and 5(c).

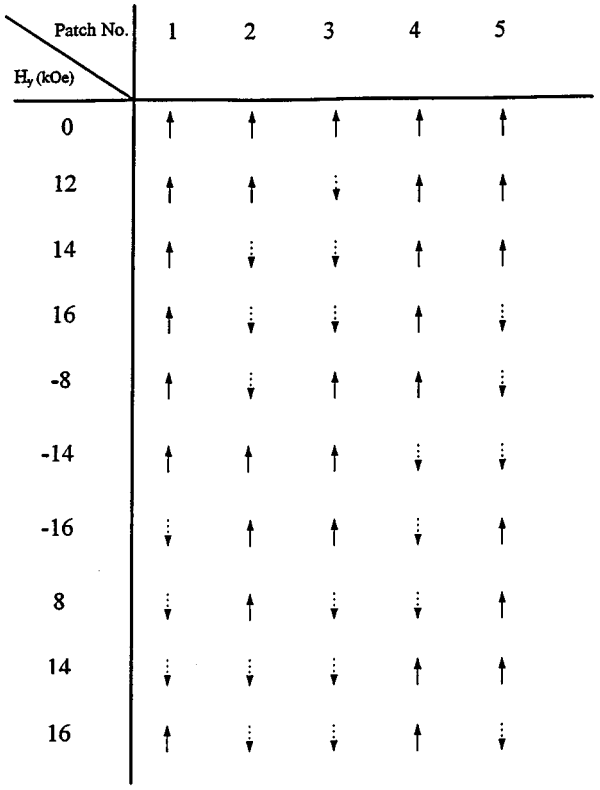

FIG. 8. Diagram showing the status of magnetization vector within each patch, corresponding to several values of the external field in Fig. 7(b). The arrows only show the directions of the Z component of the magnetic dipoles within each patch. At $H_y=0$, all the patches are magnetized parallel to $+Z$. When $H_y=12$ kOe, patch 3 reverses, and so on. Note that, after the magnetic field reaches 16 kOe, the net magnetization depends on patch 3 alone.

Figure 7(a) shows the computed loop for the case where the applied magnetic field was along Z. The vertical axis shows the normalized magnetization **M**, which has unity value when all the dipoles are along Z. At $H_z=0$, the state corresponding to Fig. 6(b), **M** has the normalized value of 0.976. When the magnetic field reaches 20 kOe, the value of **M** is equal to 0.994. This small increase of **M** with the external field agrees with the experimental data shown in Figs. 3(b) and (c).

Figure 7(b) shows the computed loop for the case where the magnetic field was applied along $+Y$. This behavior is similar to that shown in Figs. 5(b) and 5(c). The diagram in Fig. 8 shows the status of the magnetic moments within each patch, corresponding to several values of the external field

described in Fig. 7(b). The arrows only indicate whether the directions of dipoles within each patch are parallel or antiparallel to the Z axis. As the value of H_y rises from 0 to 10 kOe, the magnetization coherently rotates towards $+Y$, causing the value of **M** to drop slowly. Because patch 3 has a larger deviation from Z than the others, it is the first one to reverse at $H_y=12$ kOe. At $H_y=14$ and 16 kOe, patches 2 and 5 reverse, respectively. The reason that patch 2 reverses before patches 5 is that patch 2 is pulled by the exchange force from patch 3. When the field is reduced from $+20$ to -6 kOe, no patches reverse. Afterwards, patch 3 flips to point in the $+Z$ direction at $H_y=8$ kOe. This causes **M** to switch sign and acquire a positive value. At $H_y=-14$ kOe, it is interesting that patch 2 and 4 switch to opposite directions without changing the net magnetization of the lattice. Note, by comparing Figs. 7(b) and 8, that the net value of **M** in the hysteresis loop depends only on the status of patch 3, since the magnetizations of all the other patches cancel each other out at all values of H_y.

IV. CONCLUSIONS

In this article, we examined several obliquely deposited amorphous TbFeCo films by measuring the magnetic hysteresis loops using a Kerr loop tracer. Also, computer simulations based on the Landau–Lifshitz–Gilbert equation were employed to determine possible distributions of the easy axis. Under oblique deposition, we found the following results: (1) Distribution of the easy axes of magnetic anisotropy is asymmetric with respect to the film's normal. (2) Composition of the film shifts towards the Fe-rich side when the deposition angle increases. (3) Thickness of the film becomes small at large deposition angle.

ACKNOWLEDGMENT

We thank Mr. William McChesney of IBM Almadem Research Laboratory for preparing the samples.

[1] Y.-C. Hsieh and M. Mansuripur, J. Appl. Phys. **78**, 380 (1995).
[2] K. Wakabayashi, H. Sugiyama, T. Maeda, A. Saitou, H. Miyamoto, and H. Awano, Proceedings of SOM'94, paper MoB3 (unpublished).
[3] S. Gadetsky, T. Suzuki, J. K. Erwin, and M. Mansuripur, IEEE Trans. Magn. **31**, 3253 (1995).
[4] M. Hong, E. M. Gyorgy, and D. D. Bacon, Appl. Phys. Lett. **44**, 706 (1984).
[5] Y. Togami and N. Saito, J. Appl. Phys. **60**, 3691 (1986).
[6] F. Hellman, R. B. van Dover, and E. M. Gyorgy, Appl. Phys. Lett. **50**, 296 (1987).
[7] F. Hellman, R. B. van Dover, S. Nakahara, and E. M. Gyorgy, Phys. Rev. B **39**, 10 591 (1989).
[8] M. Mansuripur, *The Physical Principles of Magneto-optical Recording* (Cambridge University Press, London, 1995).
[9] M. Mansuripur, J. Appl. Phys. **63**, 5809 (1988).